GR24, a Synthetic Analog of Strigolactones, Stimulates the Mitosis and Growth of the Arbuscular Mycorrhizal Fungus *Gigaspora rosea* by Boosting Its Energy Metabolism[C][W]

Arnaud Besserer, Guillaume Bécard*, Alain Jauneau, Christophe Roux, and Nathalie Séjalon-Delmas

Plant Cell Surfaces and Signaling Laboratory, UMR5546 CNRS/University of Toulouse, 31326 Castanet-Tolosan, France

Arbuscular mycorrhizal (AM) fungi are obligate biotrophs that participate in a highly beneficial root symbiosis with 80% of land plants. Strigolactones are trace molecules in plant root exudates that are perceived by AM fungi at subnanomolar concentrations. Within just a few hours, they were shown to stimulate fungal mitochondria, spore germination, and branching of germinating hyphae. In this study we show that treatment of *Gigaspora rosea* with a strigolactone analog (GR24) causes a rapid increase in the NADH concentration, the NADH dehydrogenase activity, and the ATP content of the fungal cell. This fully and rapidly (within minutes) activated oxidative metabolism does not require new gene expression. Up-regulation of the genes involved in mitochondrial metabolism and hyphal growth, and stimulation of the fungal mitotic activity, take place several days after this initial boost to the cellular energy of the fungus. Such a rapid and powerful action of GR24 on *G. rosea* cells suggests that strigolactones are important plant signals involved in switching AM fungi toward full germination and a presymbiotic state.

Arbuscular mycorrhizal (AM) fungi are soil-borne microorganisms living symbiotically with most land plants and in most ecosystems (Smith and Read, 1997). They are generally highly beneficial for plant nutrition and survival, thus explaining their remarkably large ecological occurrence. They have been living in close association and have coevolved with plants for more than 400 million years (Simon et al., 1993; Remy et al., 1994). Beyond the obvious utility of studying AM symbiosis for ecological and agronomical reasons, a more fundamental interest has emerged. It is expected that several signaling mechanisms involved in the establishment of AM symbiosis have been conserved in the plant kingdom by radiation during plant evolution and that they were then exploited by more recent plant biotic interactions. Several examples of this have recently been reported, strongly suggesting that interactions between plants and nitrogen-fixing bacteria, nematodes, and parasitic plants such as *Striga* spp. and *Orobanche* spp. exploit ancestral recognition mechanisms, first developed for AM fungus symbiosis (Paszkowski, 2006; Bouwmeester et al., 2007).

AM fungi are obligate biotrophs (meaning they must get carbon from their host to complete their life cycle) and host recognition is a crucial step for their survival. Spores of AM fungi can germinate spontaneously but they will produce extremely limited hyphal growth unless they perceive the presence of a host plant. In the vicinity of host plant roots, prior to any contact, the fungus forms characteristic hyphal ramifications (Mosse and Hepper, 1975; Giovannetti et al., 1994). Its overall growth is also stimulated as is the utilization of its stored carbon (Bécard and Piché, 1989). The characteristic hyphal branching was used as a sensitive bioassay to purify and characterize active root-exuded molecules (Buée et al., 2000).

Strigolactones, previously characterized as seed germination stimulants of the parasitic plants *Striga* and *Orobanche* (Cook et al., 1966; Bouwmeester et al., 2003), were isolated and characterized as active molecules on spore germination, hyphal branching, and growth of AM fungi (Akiyama et al., 2005; Besserer et al., 2006). They have been shown to be active at subpicomolar concentrations and are suspected to play a crucial role in establishing symbiosis. Maize (*Zea mays*) plants thought to have impaired strigolactone production were shown to have fewer mycorrhizae (Gomez-Roldan et al., 2007).

In seeds of *Striga* spp. and *Orobanche* spp., the isolation of strigolactone receptors has remained elusive and their subcellular location is still unknown despite several structure-activity studies (Mangnus et al., 1992; Mangnus and Zwanenburg, 1992). In *Striga hermonthica* it was proposed that strigolactones act as elicitors of ethylene biosynthesis, leading to subsequent seed

* Corresponding author; e-mail becard@scsv.ups-tlse.fr.

The author responsible for the distribution of materials integral to the findings presented in this article in accordance with the policy described in the Instructions for Authors (www.plantphysiol.org) is: Guillaume Bécard (becard@scsv.ups-tlse.fr).

[C] Some figures in this article are displayed in color online but in black and white in print.

[W] The online version of this article contains Web-only data.

www.plantphysiol.org/cgi/doi/10.1104/pp.108.121400

germination (Logan and Stewart, 1991). In AM fungi, strigolactones were shown to induce changes in shape, density, and motility of mitochondria after 1 h of treatment (Besserer et al., 2006).

The objective of this study was to examine the role of mitochondria as an early target of strigolactone signaling and to investigate the effect of strigolactones on the fungal mitotic activity. The data support the extremely rapid and important role of mitochondria in the fungal response to strigolactones, both for energy metabolism and life-cycle control.

RESULTS

GR24 Rapidly Increases NADPH Synthesis in *Gigaspora rosea*

To monitor changes in the redox potential of cells of *G. rosea*, we carried out real-time kinetic study of NADPH in living hyphae after induction with GR24. GR24 is a chemical analog of strigolactones. Available commercially, it is a little less active than natural strigolactones (Besserer et al., 2006). The strong and characteristic autofluorescence of NADPH makes it possible to monitor fluctuations of its concentration in living cells (Chance et al., 1962; Shuttleworth et al., 2003; Cardenas et al., 2006). To minimize the nonspecific autofluorescence background, we used young germinating spores (with a maximum of two branches on the germ tube). Taking advantage of the λ-scan module of the confocal microscope, we tested the spectral specificity of the fluorescence obtained by comparing the emission spectrum of *G. rosea* treated hyphae to that of a standard NADH solution. The results plotted in Figure 1A show emission maximum at 450 nm for signals acquired from a *G. rosea* hypha before (0 min) and after (15 min) GR24 treatment. This maximum of NADH fluorescence is usually observed in living cells (Andersson et al., 1998). The 30-nm shift of the emission intensity peak with respect to the standard NADH solution has already been described as a normal phenomenon due to the cellular environment (Liang et al., 2007).

The accumulation kinetics of NADPH was then determined in the tip region of *G. rosea* hyphae treated or not with GR24 (Fig. 1B). After GR24 addition, a significant NADPH increase was observed within 5 min. Maximum intensities were reached after 10 to 15 min. This increase is followed by a stationary phase after 20 to 30 min. A slight increase of NADPH content is also visible in control hyphae, perhaps due to some experimental stress or blue light effect (Nagahashi and Douds, 2003).

To determine how NADPH fluctuations occur, we acquired fluorescence images of 115-μm-long hyphal tips, with a wide-field microscope, in a kinetics experiment (Fig. 2). The intensity of NADPH autofluorescence remained constant in control hyphae (Fig. 2, B–F) while a strong increase in fluorescence level was

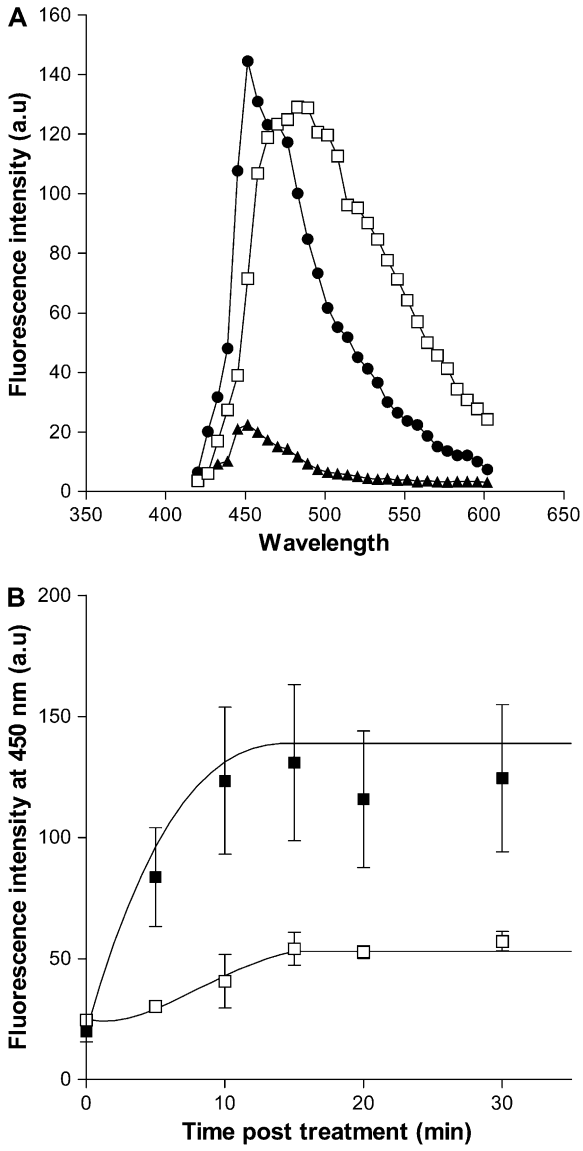

Figure 1. NADPH autofluorescence in hyphae of *G. rosea*. A, Autofluorescence emission spectra of a *G. rosea* hypha treated with 10^{-8} M GR24. Emission spectra were obtained at 405-nm excitation and recorded 0 and 15 min after treatment (black triangles and circles, respectively). They are compared with the emission spectrum of a standard NADH solution (white squares). B, Time course measurements of emission (450 nm) intensities of NADPH autofluorescence in a *G. rosea* hypha, treated (black square) or not (white squares) with 10^{-8} M GR24 and excited at 405 nm. Values are means of fluorescence signals measured in four regions (15 μm^2 each) of three hyphal tips treated in three independent experiments. Polynomial fitted curves (solid lines) are shown. Error bars are SES of the means.

observed in GR24-treated hyphae (Fig. 2, H–L). The experiment was repeated with three different hyphal tips for each treatment and very similar images were obtained. The accumulation mainly occurred within the first 20 μm behind the hyphal tip, the region of highest mitochondrial density (Supplemental Fig. S1). Fungal viability was not affected by UV illumination

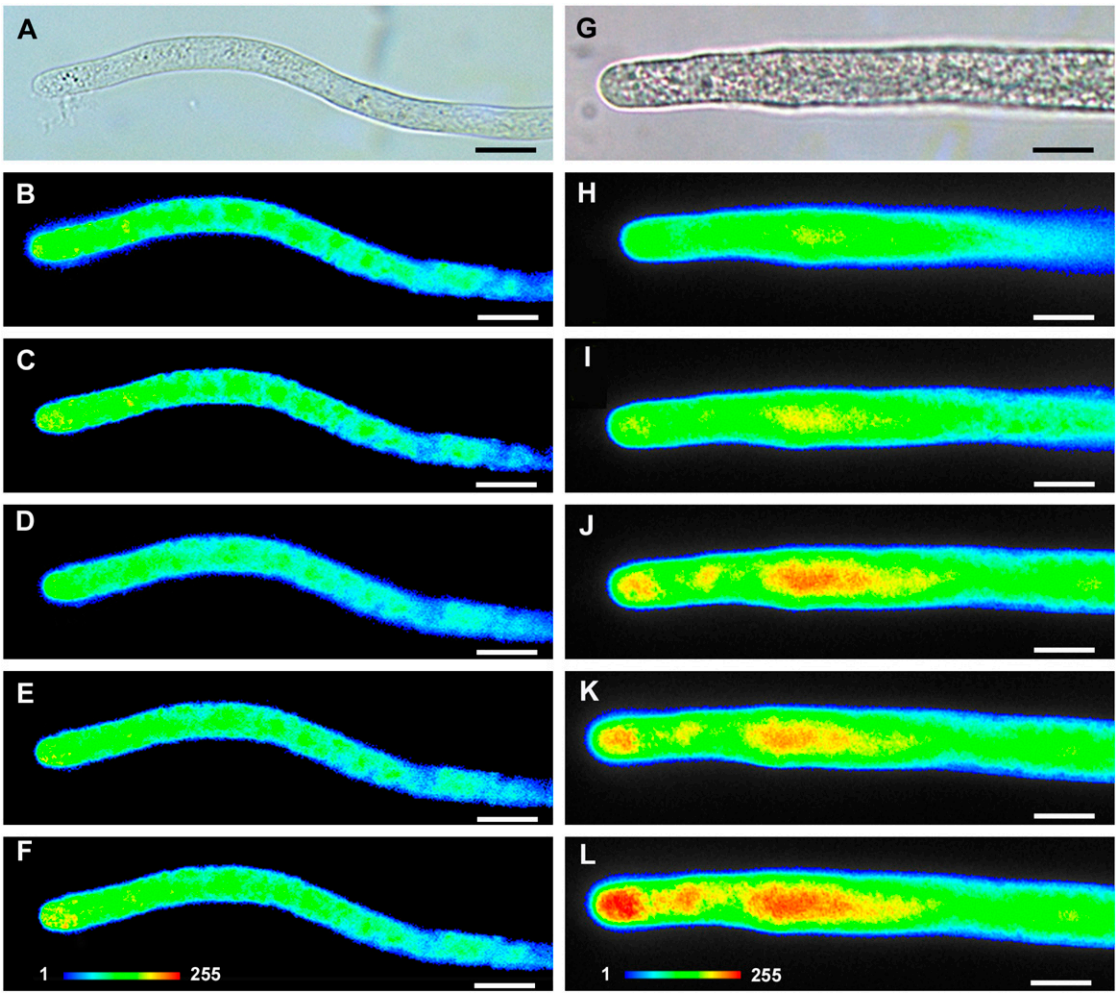

Figure 2. Time lapse sequence of NADPH autofluorescence changes after GR24 treatment. A and G, Bright-field micrographs of control (A) and GR24-treated (G) hyphae, respectively. Autofluorescence of NADPH was monitored after 0, 5, 10, 15, and 20 min, respectively, in control hyphae (B–F) and in hyphae treated by 10^{-8} M GR24 (H–L). In all pseudocolor images, the color follows convention, with red indicating high and blue indicating low levels of fluorescence signal (color intensity scale on F and L). Bars = 10 μm.

because cytoplasmic movement of vesicles and hyphal growth were still visible at the end of the experiments.

GR24 Triggers an Increase in NADH Dehydrogenase Activity

To verify that the newly synthesized NADH pool is used in the respiratory chain, we compared the activity of NADH dehydrogenase in control and treated hyphae using the cytochemical approach described by MacDonald and Lewis (1978). The basic principle of this method is that for each NADH oxidized by NADPH oxidase, electrons are transferred to nitroblue tetrazolium (NBT) which, in turn, forms blue precipitates. This allowed us to measure mitochondrial NADH dehydrogenase activity in situ at the cellular level according to the widely used histochemical method developed by Pearse (1968). Microscopic observations (Fig. 3) show that when NADH is not supplied as a substrate, only a very slight precipitate can be observed in treated hyphae (Fig. 3C) but not in controls (Fig. 3A). When NADH is supplied as a reaction substrate, formazan (NBT) precipitates form rapidly and are located near the tip, consistent with the site of the NADH accumulation observed previously (Fig. 2) and with the high apical density of mitochondria (Supplemental Fig. S1). After 20 min of incubation with exogenous NADH, the level of precipitates was higher in GR24-treated hyphae (Fig. 3D) than in the controls (Fig. 3B). This was more precisely quantified and showed a significant difference between GR24-treated and control hyphae (Fig. 3E). To make sure that the reaction is specific for NADH dehydrogenase activity, hyphae were incubated for 1 h with rotenone, a specific NADH dehydrogenase inhibitor, before treatment with GR24 or acetone. Under these conditions, only very weak

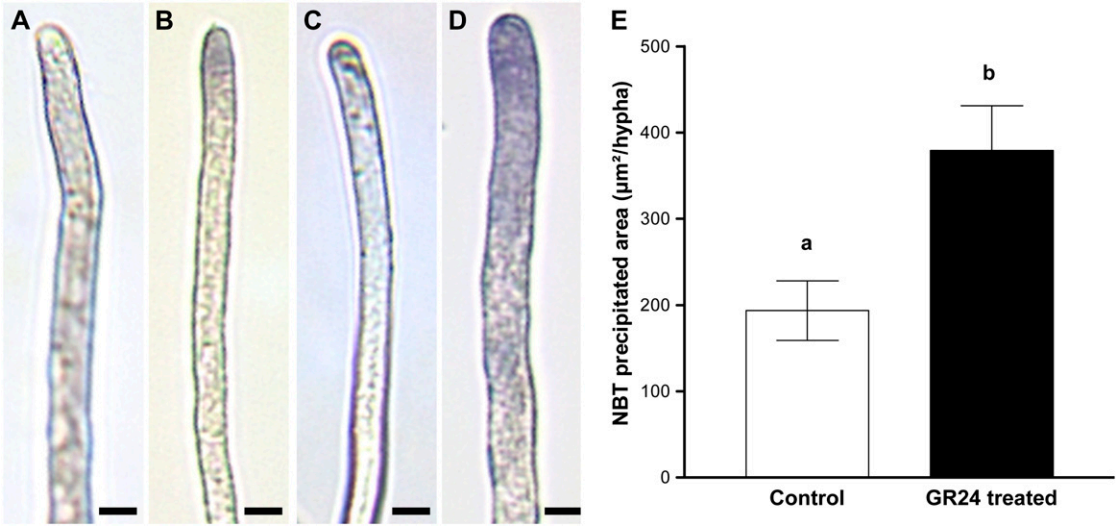

Figure 3. NADH dehydrogenase activity. A to D, Hyphae were treated 1 h with acetone (A and B) or with 10^{-8} M GR24 (C and D). They were incubated for 20 min with NBT reaction mix alone (A–C) or with NBT reaction mix supplemented with 28 mM NADH (B–D). NBT precipitates (in blue) were observed in hyphal tips (eight per treatment). Images were similar within each treatment. Bars = 5 μm. A quantitative analysis of NADH dehydrogenase activity in control (white bar) and GR24-treated hyphae (black bar), is presented (E). The conditions of incubation were as in B and D. Statistical analysis was performed with Student's *t* test ($P < 0.01$; $n = 15$). Error bars are SES of mean values. Different letters above histograms indicate that mean values from control and treated samples are statistically different.

formazan precipitates were observed (Supplemental Fig. S2).

NADH Increase Is Coupled with More ATP Production

To investigate whether oxidative phosphorylation is also induced in GR24-treated hyphae, we quantified total ATP in germinating spores of *G. rosea* treated or not with GR24 by using the luciferin-luciferase method (Lemasters and Hackenbrock, 1979). After 1 h, GR24-treated hyphae presented an approximately 30% higher ATP content (Table I). This result, showing an activation of fungal oxidative phosphorylation, is consistent with a higher NADH content and NADH dehydrogenase activity. We can therefore conclude that the overall energy metabolism of the mitochondria, including ATP synthesis, is strongly and rapidly enhanced in *G. rosea* treated with GR24.

Early Mitochondrial Response to GR24 Does Not Require Transcriptional Induction

It has been shown previously that the semipurified root exudate fraction (the so-called branching factor; Nagahashi and Douds, 1999, 2000, 2007; Buée et al., 2000) affects the expression of genes with a mitochondrial function (Tamasloukht et al., 2003, 2007). The rapid (within minutes) mitochondrial activation of *G. rosea* by GR24 that we observed suggests that it does not rely on enhanced transcription. Nevertheless, we tested whether the synthetic strigolactone GR24 could, by itself, induce gene expression that parallels mitochondrial and cell activation. Thus, the expression of various genes coding for proteins involved in mitochondrial metabolism and growth was monitored by a real-time quantitative PCR approach. The genes chosen were nuclear genes isolated from an EST library (A. Besserer and N. Séjalon-Delmas, unpublished data) and by homology searches. They are putatively assigned to genes involved in oxidative phosphorylation (ATP synthase subunit-α, accession [AC] no. EX452304; cytochrome *c* oxidase V, AC no. EX452353), cell architecture (α-tubulin, AC no EX452542), cell fate (sphingosine-1P lyase, AC no. EX452498), primary metabolism (pyruvate carboxylase, AC no. AJ419670; 3-ketoacyl-CoA thiolase, AC no. EX452332), ROS detoxification (CuZn superoxide dismutase, AC no. AJ640199; Lanfranco et al. 2005) and 40S nuclear subunit export protein (NOC4, AC no. AJ419666).

In a first experimental design, transcript profiles of the chosen genes were analyzed after a short stimulation of pregerminated spores (6-d): 1, 5, 24, or 48 h with GR24 or 0.0001% acetone. Normalization with α-tubulin was used in this first set of experiments. Preliminary experiments showed that α-tubulin expression was not different between control and treated samples, in the time course between 1 and 48 h (average of threshold cycle [CT] 23.9, SD = 0.8, $n = 12$). No change in expression of the selected genes was observed in the three biological replicates although the hyphal branching response could be observed after 24 h of treatment, as expected (data not shown). This suggested that the rapid cellular GR24 responses described above were not transcriptionally regulated but were rather the result of some posttranscriptional regulation.

Table I. *Effect of GR24 treatment on ATP content in G. rosea*

ATP was quantified using the luciferin-luciferase method, and protein amount was determined using standard BCA protocol (see "Material and Methods"). Values are the mean of three replicates in each experiment, ± SE of the mean. In each experiment, the difference of ATP concentrations between GR24-treated and control hyphae are significant (Student's *t* test $P < 0.05$).

	GR24-Treated	Control	Relative ATP Increase
	pmol mg^{-1} *protein*	*pmol mg*$^{-1}$ *protein*	
Experiment 1	1265.70 ± 22.26	971.30 ± 89.24	30%
Experiment 2	596.66 ± 27.69	437.33 ± 29.36	36%
Experiment 3	1713.32 ± 36.96	1359.19 ± 49.02	26%

In a second set of experiments, where the spores were germinated in the presence of GR24 for 2, 5, and 10 d, the expression of each chosen EST was quantified by real-time quantitative reverse transcription (RT)-PCR in hyphae and spores. Gene expression changes for each time point was calculated by using the NOC4 homolog as a reference gene because differences in α-tubulin expression here were noted. NOC4 is constitutively and ubiquitously expressed in mammals (Bachman et al., 1999) and its transcription level was not affected in our experimental conditions (average of CT 27.5, SD = 1.05, $n = 18$). It was therefore used as our reference gene for the ΔΔCT calculation (Livak and Schmittgen, 2001; Nolan et al., 2006).

Because the expression profiles were similar in spores and hyphae (data not shown), both at 5 and 10 d, only the expression profiles in hyphae are shown (Fig. 4). After 2 d in the presence of GR24, no modifications of gene expression were observed (data not shown on graph), which is consistent with the fact that GR24 has no effect on *G. rosea* spore germination (Besserer et al., 2006). After 5 d of GR24 exposure, transcription of nearly all genes was activated by a factor ranging from 1.5 to 4. More careful examination of gene expression data after 5 d of treatment indicates that the putative pyruvate carboxylase gene was not induced whereas the putative ketoacyl thiolase gene was induced by a factor of 1.9. This result is consistent with the fact that these two enzymes act in opposite metabolic pathways, neoglucogenesis and β-oxidation of fatty acids, respectively. In parallel, putative genes involved in mitochondrial oxidative phosphorylation such as cytochrome *c* oxidase V and ATP synthase, were up-regulated (1.9- and 4.0-fold, respectively). The putative CuZnSOD gene was also up-regulated by a factor of 2.0 in response to GR24. One of the most up-regulated genes was the putative α-tubulin gene (3.2-fold). These results suggest that in response to GR24, the genes involved in catabolism, mitochondrial metabolism, and cell architecture were up-regulated.

After 10 d of GR24 exposure, the transcriptional level of the same genes returned to the level of the constitutive reference gene, NOC4, except for the putative ATP synthase gene, which remained higher than the control (1.5-fold). This suggests that most of the transcriptional regulation observed at 5 d is transient and reflects the boost of energy, which is necessary for the branching response to GR24.

Nuclear Division Was Stimulated in GR24-Treated Hyphae

To test the hypothesis that GR24 activates nuclear division, as observed by Buée et al. (2000) in response to root exudates, we counted the nuclei in three separate zones of the fungus: the hyphal tips, the mycelial body, and the spores. Nuclear staining of hyphal tips was performed with acridine orange (AO). In GR24-treated hyphae, an accumulation of nuclei was observed in the apical zone (Fig. 5). Quantitative analysis showed that the number of nuclei in GR24-treated hyphal tips was 2-fold higher than in the control.

Nuclear staining of the mycelial body was performed with diaminophenylindole (DAPI). It showed that the nuclear distribution in any randomly chosen hyphal segment (excluding the tips) remained constant (about 10 nuclei per 100 μm) and was not affected by GR24 treatment (Supplemental Fig. S3). Measurement of hyphal elongation in response to GR24 or acetone treatment showed that treated hyphae were longer than control hyphae (170.07 mm versus 59.19 mm). Because nuclei distribution was not affected by GR24 treatment, we concluded that treated germinating hyphae had a higher total number of nuclei.

To make sure that the greater number of nuclei was not due to a more active migration of preexisting nuclei from the spore, we estimated, by quantitative PCR, the remaining genomic DNA in the spores (hyphae removed), treated or not, after 5 d of germination. Amplifications were performed on putative α-tubulin and NOC4 genes. Gene copy numbers were determined by absolute quantification, using the corresponding PCR products to plot the calibration curves (Fig. 6). Similar results were obtained with the two genes, thus validating the methodology (Fig. 6A). The nuclei remaining in the spores were also counted directly under the fluorescence microscope using the method of Bécard and Pfeffer (1993; Fig. 6B). In both molecular and microscopic approaches, no significant differences were noted in gene copy or nucleus number between treated samples and control. This rules out the hypothesis that the overall higher number of nuclei in treated germinating hyphae was the result of more nuclear migration from spores. Thus, the increase in nucleus number in the hyphal tips and the greater total number of nuclei in the mycelial body strongly supports the hypothesis that, in *G. rosea*, GR24 also induces mitosis. This is consistent with previous observations on *G. gigantea* (Buée et al., 2000) where nuclear division was induced by root exudates.

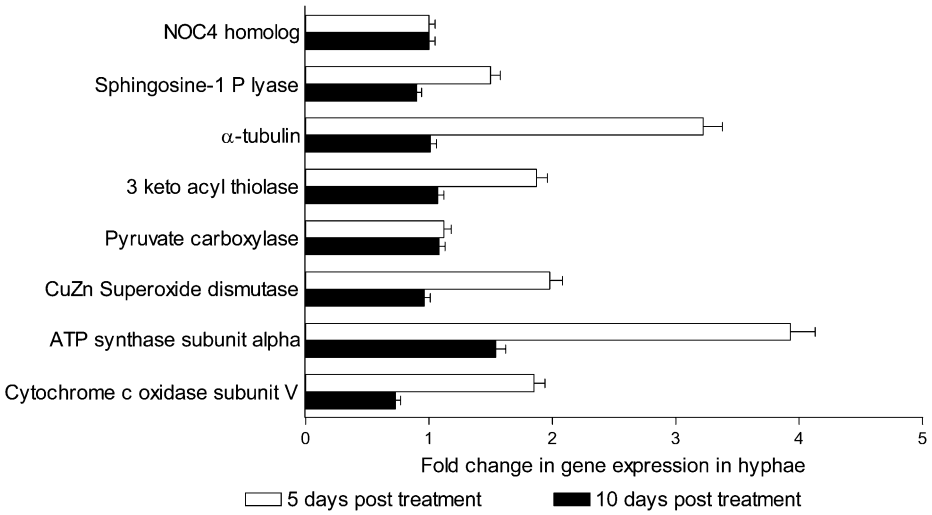

Figure 4. Effect of GR24 on gene regulation. Real-time RT-PCR was carried out on total mRNA extracted from GR24-treated hyphae after 5 and 10 d of treatment. Total RNA yield was measured and cDNA synthesis performed as described in the experimental procedures section. Relative nuclear gene expression in GR24-treated hyphae was compared to acetone-treated controls. Expression of each gene was obtained using the $2^{-\Delta\Delta CT}$ method with NOC4 as the reference gene (see details in text). Data are the means of two independent experiments.

DISCUSSION

Mitochondrial Energy Metabolism Is Fully and Rapidly Activated in Response to GR24

Strigolactones have been previously shown, in AM fungal cells, to induce a rapid (1 h) increase in O_2 consumption and strong changes in mitochondrial density, shape, and movement (Besserer et al., 2006). The first objective of this study was to verify that the strigolactone activation of mitochondria actually leads to the activation of oxidative phosphorylation. An increase of oxygen consumption does not necessarily reflect activation of ATP synthesis but can be the result of uncoupling of the electrochemical gradient of protons across the inner mitochondrial membrane and ATP synthesis (Marcinek et al., 2004). Higher O_2 consumption can also be the result of a stress response (Popov et al., 2001; Calegario et al., 2003). We determined that GR24 treatment triggers strong NADPH accumulation in hyphal tips, which is correlated with an increase of NADH dehydrogenase activity. After 1 h of treatment, more ATP was produced (30% increase). This demonstrates that the mitochondrial changes observed by Besserer et al. (2006) are closely linked with an overall activation of oxidative phosphorylation in the fungus. In eukaryotic cells, ATP production is highly regulated by energy needs (Devin and Rigoulet, 2007). Thus, the 30% increase in ATP production suggests intense energy demand in *G. rosea* hyphae that could coincide with the switch from asymbiotic to presymbiotic growth, the latter being characterized by greater hyphal growth (which lasts weeks instead of days) and more intense hyphal branching.

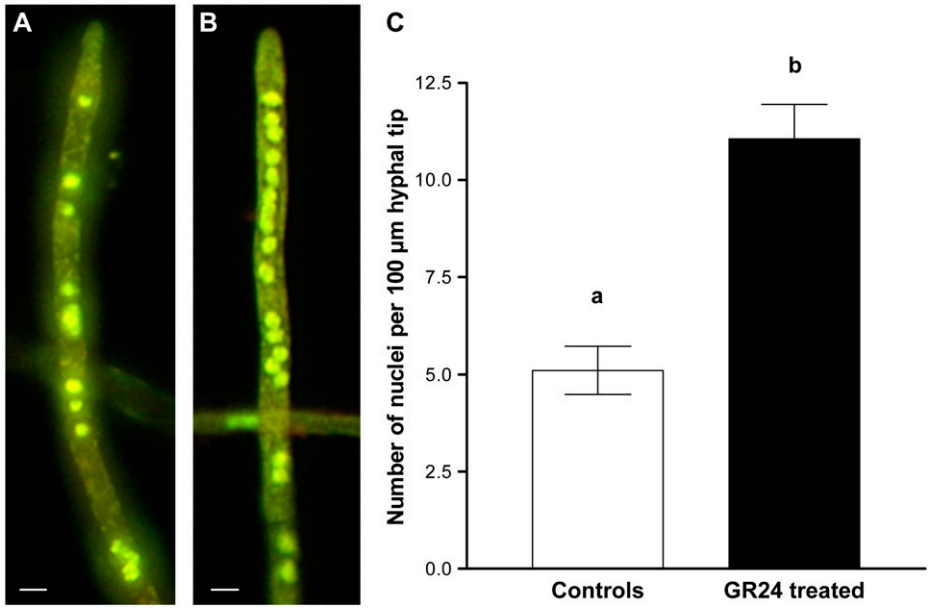

Figure 5. Effect of GR24 on the number of nuclei in *G. rosea* hyphal tips. A and B, Fungal cells treated with 0.0001% (A) or 10^{-8} M GR24 (B) were stained with AO after 5 d. Bars = 10 μm. C, After each treatment, nuclei were counted in the first 100-μm segment of 18 hyphal tips. Different letters above histograms indicate a significant difference between the mean values (Student's *t* test, $P < 0.001$; $n = 18$). Error bars are SES of mean values. [See online article for color version of this figure.]

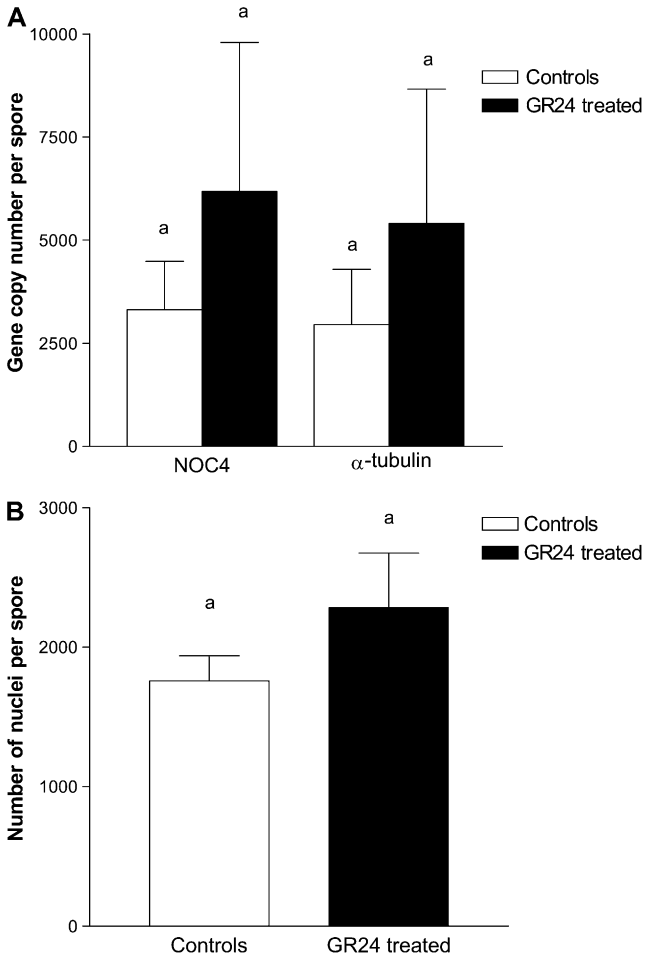

Figure 6. Effect of GR24 on spore nucleus number. Spores were incubated in the presence of 10^{-8} M GR24 (black bars) or 0.0001% acetone (white bars) for 5 d. A, Using five spores (germinated hyphae removed) per DNA extraction, real-time PCR absolute quantification was carried out on putative α-tubulin and NOC4 homolog genes. The copy number per spore was determined as described in "Materials and Methods." Bars are means ± SE of seven replicates. For both genes, there was no significant difference between control and treated spores ($P = 0.57$). B, Direct quantification of the nucleus number in crushed spores (10 spores per treatment) and mithramycin staining, showing no significant difference between control and treated spores (Student's t test, $P = 0.24$; $n = 10$). Error bars are SE of mean values.

A second objective of this study was to better characterize the way strigolactones regulate fungal mitochondrial activity. The higher mitochondrial density and protein content observed by Besserer et al. (2006) were interpreted as an enhancement of mitochondrial biogenesis. In yeast and animal cells mitochondrial biogenesis typically occurs when cells must meet higher energy demands and is considered as a long-term adaptation (Devin and Rigoulet, 2007). More rapid mitochondrial responses have also been characterized that include activation of matricial dehydrogenases (e.g. pyruvate dehydrogenase) and of ATP synthase (McBride et al., 2006). This kind of regulation requires Ca^{2+}-mediated events of protein phosphorylation/dephosphorylation (Hopper et al., 2006). In our study, GR24-treated cells exhibited enhanced NADPH concentration and NADH dehydrogenase activity within 5 to 20 min. These rapid responses strongly suggest that strigolactone activation of *G. rosea* mitochondria also occurs via short term regulation, conceivably through posttranslational regulation of some key enzymes. As it has been shown that a rapid change of mitochondrial redox status could reflect catabolic metabolism activity (Mayevsky and Rogatsky, 2007); it is tempting to speculate that the increase in NADH that we observed after GR24 treatment is fueled by lipid catabolism. We found that the strongest mitochondrial response to GR24 was localized in the hyphal tips, as shown with MitoTracker Green staining of mitochondria, the NADH autofluorescence, and NBT staining of the NADH dehydrogenase. Interestingly, this can be correlated to previous observations made in *G. rosea* in response to root and root exudates, also located in the hyphal tip region, such as the activation of plasmalemma H+-ATPase and the elevation of cytosolic pH (Lei et al., 1991; Jolicoeur et al., 1998, Ramos et al., 2008).

GR24 Late Action on Gene Expression

The rapidity of the first mitochondrial responses (within 5 min) to GR24 suggests that specific transcriptional regulation is not required. Accordingly, we observed no variation in the expression of the various selected genes during the first 48 h of treatment (spores pregerminated or not). Transcript levels were strongly (53-fold) increased in spores after 2 d of incubation (not shown data), but this induction occurred independently of GR24 treatment as a first manifestation of germination (Beilby, 1983). Although our gene-targeted approach does not allow us to exclude specific and early gene induction at the nuclear or mitochondrial level, our results suggest that during the first hours of GR24 treatment, regulations that will lead to greater hyphal branching are mostly posttranscriptional. Although, a previously isolated root exudate fraction, and here the synthetic strigolactone (GR24), have been shown to induce similar effects on mitochondrial changes (Tamasloukht et al., 2003; Besserer et al., 2006), the results on gene expression are different. The rapid up-regulation of several genes observed in response to root exudates (Tamasloukht et al., 2003, 2007) suggests that other, yet unknown, molecules act in synergy or in parallel with strigolactones (Nagahashi and Douds, 2007).

G. rosea requires 5 d of incubation in the presence of GR24 before exhibiting a significantly higher hyphal growth rate (Besserer et al., 2006). We observed that most of the selected genes also required 5 d of treatment to be up-regulated and that they were no longer up-regulated after 10 d. If 5 d is the starting point of an increase in hyphal growth rate, 10 d coincides with the return to a normal growth rate (Besserer et al., 2006). We hypothesize that the up-regulation of gene expres-

Table II. *Sequences of primers used in this work*

Gene	Primer Sequence (5′-3′)	Strand
α-Tubulin	CTACACCGAGGGTGCTGAACTT	Forward
	GAGTGGGTTATTTGGAAACCTTGT	Reverse
Sphingosine-1P lyase	GCATCTGTGGTAGCATTTGG	Forward
	CCGCTGGTGGATTTTGTAAT	Reverse
NOC4 homolog	GCAGGTCTCCGTTTACGCTAA	Forward
	TGGCCAAAAGGAGGCAATT	Reverse
Pyruvate carboxylase	TCCGGGTTATGGTTTCCTTTCGGA	Forward
	TCAATAACATCAGGTGTAGGACCAACAAA	Reverse
CuZn superoxide dismutase	GCTGGACCTCATTTCAATCCAC	Forward
	TGTTCTTTAGCAACGCCATTCAC	Reverse
ATP synthase	TAGATCCGCCACCATTATCC	Forward
	CTTTGTTGCTTCGTCGTCCT	Reverse
3-Ketoacyl-CoA thiolase	TTTATTCGTGCTTCAGTTGTTG	Forward
	TTGATTCCAAGTCCAGTTCG	Reverse
Cytochrome *c* oxidase V	CAGCATCTTTGGCTTCCTTT	Forward
	GCTTTCTGACGACGCATTTT	Reverse

sion observed after 5 d allows the synthesis of the proteins required for this increase in hyphal growth rate. Among our selected genes, those up-regulated at 5 d are putatively involved in mitochondrial metabolism (ATP synthase and cytochrome *c* oxidase V) and in cell proliferation (α-tubulin and sphingosine-1P lyase). Activation of CuZnSOD has already been reported in *Gigaspora margarita* in response to *Lotus japonicus* root exudates (Lanfranco et al., 2005). Absence of regulation of putative pyruvate carboxylase and up-regulation of putative 3-ketoacyl-CoA thiolase strongly suggest an increase of lipid catabolism rather than neoglucogenesis. Stimulation of this catabolic pathway would provide a higher amount of acetyl-CoA and accelerate the citric acid and glyoxylate cycles, leading to higher NADPH and ATP synthesis required for more active anabolism.

The Mitosis of *G. rosea* Is Also Stimulated in Response to GR24

The fact that GR24-treated *G. rosea* produced a larger hyphal network, and that the mycelial body presented an unaltered distribution of nuclei, together with the assessment that the observed hyphal nuclei did not already exist in the spore, indicated that an overall higher number of nuclei was present in the treated fungus. In filamentous fungi most mitotic activity occurs at the hyphal tip, where most apical growth is sustained (Horio and Oakley, 2005; Steinberg, 2007). Accordingly, we observed an accumulation of twice as many nuclei in the apical area of the GR24-treated hyphae. The fungal apical growth model (Steinberg, 2007) underlines the strong needs in energy and mRNA in this short region behind the tip that could explain the accumulation of both mitochondria and nuclei in this area. It remains to elucidate whether the apical mitochondria, in addition to providing energy, also play a role as a signaling platform for cell cycle progression (Mandal et al., 2005).

What Perception System Is Involved in the Strigolactone Signaling?

AM fungal response to strigolactone presents some striking convergences with the germination induction process of parasitic plant seeds in response to GR24, such as the requirement for several days of conditioning for responsiveness capability to GR24 (Joel et al., 1995) or the very short exposure time (5 min) required for a physiological response to this molecule (Gonzalez-Verdejo et al., 2005). Like for any plant seed, early mitochondrial activation must also occur during the induction of germination of parasitic plant seeds.

How strigolactones act on parasitic seeds of *Striga spp.* and *Orobanche spp.* is still poorly understood (Bouwmeester et al., 2007). Nevertheless, it has been shown that ethylene stimulates germination of *Striga* spp. seeds in the absence of the host plant (Parker, 1991). In addition, root exudates of the host plant, as well as strigol and GR24 have been shown to be able to trigger ethylene biosynthesis in *Striga* seeds (Logan and Stewart, 1991, Babiker et al., 1993; Sugimoto et al., 2003). More generally ethylene is known to stimulate seed germination of plants (Abeles and Lonski, 1969). Endogenous synthesis of ethylene was correlated with the breakdown of lipid reserves and an increase of mitochondrial density during seed germination of *Ricinus zanzibarensis* (Spencer and Olson, 1965). Thus, in seeds (as in climacteric fruits), ethylene enhances mitochondrial metabolism (Navet et al., 2003). These arguments support the hypothesis of Logan and Stewart (1991) who proposed that germination stimulants of seeds of *Striga* spp. and *Orobanche* spp. trigger germination by promoting ethylene biosynthesis. An interesting hypothesis would be that, similarly, AM fungi respond to strigolactones via an enhancement of endogenous ethylene synthesis, which then stimulates mitochondrial metabolism.

Strigolactones could also first target mitochondrial or cytoplasmic receptors, as do thyroid hormones in mammalian cells that stimulate mitochondrial biogen-

esis, lipid catabolism, and respiration (Scheller and Sekeris, 2003; Weitzel et al., 2003). It was also proposed in the seed of the parasitic *Orobanche* that strigolactones bind plasmalemma receptors, establishing a covalent link (Humphrey and Beale, 2006).

More work is required to determine how strigolactones are perceived in AM fungal and parasitic plant systems and whether this perception is similar or not.

MATERIALS AND METHODS

Fungal Material

Spores of the AM fungus *Gigaspora rosea* (DAOM 194757) were routinely produced on leeks and collected by wet sieving. They were washed in 0.05% (v:v) Tween 20, soaked with 2% (w:v) chloramine-T (Sigma) for 10 min, washed again three times in sterile water, and stored in an antibiotic solution containing 100 mg L^{-1}gentamycin and 200 mg L^{-1} streptomycin. After 5 d at 4°C, a second treatment with chloramine-T was carried out as mentioned above.

Spores of *G. rosea* were pregerminated on solid (0.4% Phytagel; Sigma) M medium, without Suc, for 5 to 6 d. Five microliters of 10^{-8} M GR24 were injected in two wells dug on each side of the germ tube. Hyphal elongation was measured during 5 d according to Besserer et al. (2006)

Chemical

The strigolactone analog GR24 was purchased from Chiralix and was used in aqueous solution at 10^{-8} M from a 10^{-2} M stock solution in acetone. A 0.0001% solution of acetone was used as a solvent for the control test.

NADH Autofluorescence

Surface-sterilized spores of *G. rosea* were incubated in liquid M (Bécard and Fortin, 1988) medium for 3 to 4 d at 30°C in the dark under 2% CO_2. Germinating spores exhibiting germ tubes with 2 to 3 hyphal branches were carefully mounted on a glass slide for microscopic observation. Emission spectra of NADH autofluorescence were obtained on a Leica confocal microscope using a 63× objective (water immersion, 1.2 numerical aperture). Fungal cells were treated directly under the microscope by introducing 10 μL of 10^{-8} M GR24 underneath the coverslip. Emission spectra (430–600 nm) were obtained by λ-scan mode on fungal cells excited at 405 nm with a laser diode (Wu and Qu, 2006). The hardware parameters were the following: acousto-optical tunable filter at 45%; photomultiplier tube at 842 V; scan speed 400 Hz for all acquisitions. Emission spectra were acquired after 0, 5, 10, 15, 20, and 30 min of treatment (less than 1 s per acquisition). UV pulse was restricted to image acquisition to avoid cell damage. Autofluorescence emission spectra of 10 μM standard NADH solutions were obtained under the same conditions.

Visualization of the NADH fluorescence signal in fungal cells was achieved on an inverted wide-field fluorescence microscope (Leica). A DAPI filter (excitation, 340–380 nm; emission LP 425 nm) was used for proper signal selection. Germinating spores were treated under the microscope as described above with 10 μL of 10^{-8} M GR24 or with 0.0001% acetone for controls. Images were acquired with a CCD camera (Color Coolview; Photonic Science) after 0, 5, 10, 15, and 20 min of treatment, using a 63× immersion oil objective with numerical aperture 1.32. UV pulse was restricted to image acquisition to avoid cell damage. Hyphal viability was assessed after each experiment by visualizing vesicular movement. False color fluorescence intensity images were processed with Image Pro Plus software (Media Cybernetics).

Mitochondria Staining

Mitochondria were stained with MitoTracker Green FM (Invitrogen-Molecular Probes) as previously described (Besserer et al., 2006). Briefly, after 5–6 d of germination in liquid M medium, germinating spores were incubated with the dye (1 μM) for 2 h at 30°C in the dark under 2% CO_2. During the staining process, germinated spores were treated with 10^{-8}M GR24, or v:v acetone (control) for 1 h. After treatment, germinated spores were washed with liquid M medium, mounted on glass slides, and observed using an inverted microscope (Leica DMIRBE; excitation, 450–490 nm; emission, 515 nm). Images were acquired with a CCD camera (Color Coolview; Photonic Science) using a 40× immersion oil objective.

NADPH Dehydrogenase Activity

NADPH dehydrogenase (EC 1.6.99.3) activity was detected in situ as previously described (MacDonald and Lewis, 1978; Peltier and Schmidt, 1991). Briefly, a stock solution of 4 mg mL^{-1} NBT (Promega), Tris-HCl buffer (0.2 M pH 7.4), $MgCl_2$ (5 mM), and H_2O UHQ made up to 9 mL was prepared. Staining solution was obtained by adding 9 mL of the stock solution to 1 mL of NADH solution at 20 mg mL^{-1}. After 6 d of germination in liquid M medium at 30°C in the dark under 2% CO_2, spores of *G. rosea* were treated with 10^{-8} M GR24 or 0.0001% acetone for 30 min at 30°C in the dark under 2% CO_2, and transferred immediately into the staining solution for 20 min. Samples were washed twice in phosphate-buffered saline (PBS) buffer (pH 7.4) and mounted on glass slides for observation (eight hyphal tips per treatment). The observations were performed on an inverted wide-field fluorescence microscope (Leica) under direct light using a 40× long-distance objective with a numerical aperture of 0.55. Quantification of formazan precipitates was carried out at the tips of germ tubes. Ten germinating spores (one germ tube per spore) were treated (10^{-8}M GR24 or 0.0001% acetone) in each experiment (five spores per treatment). Three experiments were carried out. Experimental reproducibility was assessed by one-way ANOVA and showed no significant difference ($F = 1.62$; $P = 0.21$). This allowed us to pool the data for calculation of the means ($n = 15$). Quantification of apical NBT precipitates was computed with Image Pro Plus software and statistical analysis with SPSS software (SPSS). Using the same experimental design, specificity of the reaction was assessed with a preincubation of hyphae for 1 h in the presence of 20 μM rotenone.

Measurement of Cellular ATP Content

Cellular ATP level was measured with the luciferin/luciferase assay (Lemasters and Hackenbrock, 1979) using the CellTiter-Glo luminescent cell viability assay kit (Promega). After 6 d of germination, pools of 40 spores of *G. rosea* were treated for 1 h with 10^{-8}M GR24 or with 0.0001% acetone. They were then ground in a microcentrifuge tube with 100 μL of Cell Titer Glo buffer (Promega) and centrifuged at 8,000*g* for 2 min. The supernatants were separated into two parts of 50 μL. An equal volume (50 μL) of CellTiter reagent (Promega) was added for ATP luminescence measurement. After 10 min of incubation at room temperature, 90 μL of the reaction mix was transferred into a luminometer (type 1250; Bio-Orbit) tube and luminescence was recorded every second for 1 min. Conversion of luminescence to ATP concentration was achieved by comparison to a standard ATP curve with concentrations ranging from 0 to 15 μM. The remaining 50 μL of supernatant was used for total protein quantification. The standard bicinchoninic acid (BCA; MicroBCA protein assay kit; Pierce Rockford) microplate protocol was used. The calibration curve was established in duplicate using a bovine serum albumin dilution series from 0 to 750 μg mL^{-1}. Compatibility between CellTiter-Glo buffer (Promega) and BCA quantification was tested to ensure linearity of measurement (Betz, 2007). Proteins were estimated in each sample using 20 and 10 μL of supernatant. In each sample, ATP content was normalized with respect to total protein content resulting in a relative ATP content. Three biological experiments were carried out independently. A Student's *t* test was applied for each experiment.

Nucleus Staining

For nucleus counting in hyphae, AO and DAPI were used. Prior to staining with either of the stains, spores of *G. rosea* were incubated for 5 d in liquid M medium with 10^{-8} M GR24 or 0.0001% acetone at 30°C in the dark under 2% CO_2. AO was used to stain the hyphal tip nuclei. It interacts with DNA or RNA by intercalation or electron attraction in living cells. When AO is intercalated, DNA emits green fluorescence (525 nm) at 488 nm excitation. For each treatment, 18 hyphal tips produced by 18 spores were stained with 0.1 μg μL^{-1} AO (Invitrogen-Molecular Probes) for 5 min in PBS buffer, pH 7.4. After staining, samples were washed three times in PBS buffer, pH 7.4. DAPI (1 μg mL^{-1}) was used directly on a glass slide to stain the nuclei of the general mycelial body (each treatment used 10 spores). After DAPI staining, DNA emits blue fluorescence (461 nm) at 358-nm excitation. Observations and image acquisition were performed on an inverted wide-field fluorescence

microscope (Leica) using a 40× long-distance objective (numerical aperture of 0.55) for AO staining and a 10× objective (numerical aperture of 0.22) for DAPI staining. The filters used were: excitation 450 to 490 nm and emission 515 nm for AO; excitation 340 to 380 nm and emission 425 nm for DAPI. Nuclei in the first 100 μm behind the hyphal tips and nuclear concentration in mycelial body were counted with Image Pro Plus software (Media Cybernetics). Statistical analysis was performed with SPSS software on 18 spores for each treatment. For counting nuclei still present in germinating spores, treated or not for 10 d with 10^{-8} M GR24, the DNA-specific stain mithramycin A was preferred (Bécard and Pfeffer, 1993). Ten spores for each treatment were crushed on a glass slide in 100 μg mL^{-1} mithramycin A dissolved in 15 mM $MgSO_4$. Microscopic observations were carried out immediately. Observations were performed on an inverted wide-field fluorescence microscope (Leica; excitation, 450–490 nm; emission 515 nm) using a 20× long-distance objective with a numerical aperture of 0.40. Nucleus counting was carried out as previously described by Bécard and Pfeffer (1993) with Image Pro Plus software.

Quantification of Spore DNA

Eight independent batches of 40 spores were germinated for 5 d in the presence of 10^{-8} M GR24 or 0.0001% acetone at 30°C in the dark and under 2% CO_2. The spores and hyphae were then separated under a stereomicroscope before DNA extraction. Spore DNA extraction was performed with the genomic wizard DNA isolation kit (Promega) including an RNase treatment step, dividing by three the extraction volumes recommended by the manufacturer. Final elution was in 20 μL of UHQ water. Extracted DNA was tested for absence of foreign fungal DNA contamination by amplification of the ITS ribosomal region with ITS1/ITS4 primers (Gardes and Bruns, 1993). Only one amplicon was obtained at 500 bp corresponding to the expected size of the *G. rosea* amplicon (Redecker et al., 1997). Putative α-tubulin and NOC4 homolog genes were amplified by PCR and corresponding amplicons were purified using Wizard SV Gel and the PCR Clean-Up System (Promega) according to the manufacturer's instructions. Purified amplicons were quantified with an ND-1000 spectrophotometer (Nanodrop Technologies). Taking into account the amplicons' size and the weight of 1 bp (660 D), DNA concentrations were converted into copy numbers. These amplicons were diluted from 10^{10} to 10^7 copies to carry out a calibration curve. Efficiency of amplification was then determined for each amplificate according to the $E = 10^{-1/\text{slope}}$ (Pfaffl, 2001) equation and was above 1.75. DNA extracted from spores treated with GR24 or with acetone, diluted from 0.15 to 15 ng, gave similar amplification efficiency to that of amplificates used for the calibration curve.

RNA Extraction

In a first experimental design, spores were grown for 6 d at 30°C in the dark under 2% CO_2 and then treated with 10^{-8} M GR24 or 0.0001% acetone for 1, 5, 24, or 48 h. Culture medium was removed and germinating spores were frozen in liquid nitrogen. In a second experimental design, spores were incubated for 0, 2, 5, or 10 d in liquid M medium at 30°C in the dark under 2% CO_2 in the presence of 10^{-8} M GR24 or 0.0001% acetone. After 5 and 10 d of germination, hyphae were separated from germinated spores under a stereomicroscope. They were immediately frozen in liquid nitrogen. For each induction time, 200 germinated spores of *G. rosea* were used. Total RNA was extracted with RNAeasy plant mini-kit (QIAGEN). To remove residual genomic DNA, RNA was treated with RNase-free DNase (Invitrogen) according to the manufacturer's instructions.

Real-Time Quantitative RT-PCR

Total RNA yield and concentration was measured with an ND-1000 spectrophotometer and the concentration was adjusted to 75 ng μL^{-1} in each sample. The integrity of the RNA was evaluated with an Agilent 2100 bioanalyzer (Agilent Technologies). To reverse the transcription step, ImPromII enzyme (Promega) was used according to the manufacturer's instructions. First, strands of cDNA were purified and concentrations of final working solutions were adjusted according to the ND-1000 spectrophotometer quantification. Real-time PCR was carried out in optical 384-well plates using the ABI Prism 7900 HT sequence detection system (Applied Biosystems). Amplifications were carried out in 10 μL of reaction volume containing 5 μL of SYBR Green PCR MasterMix 2× (Applied Biosystems), 10 μM each primer (final concentration) and 5 ng of cDNA template. Each gene amplification was carried out in triplicate. Triplicates were validated when technical error was under 0.5 CT. The PCR program was 50°C for 2 min, 95°C for 10 min, 40 cycles at 95°C for 15 s, and 60°C for 1 min. Analyses of melting curves were performed after each reaction to exclude nonspecific amplifications. The optimal baseline and threshold values were determined using the automatic CT function available with SDS 2.2 software (Applied Biosystems). Amplification efficiency (E) was determined for all primers with the equation: $E = 10^{-1/\text{slope}}$ (Pfaffl, 2001) and all were >1.75, after template dilution from 0.15 to 15 ng. Putative α-tubulin was used for normalization in the first experimental design (expression profiling up to 48 h after treatment). Real-time amplifications were carried out with the same amounts of cDNA. No variation in the expression level (CT) of the α-tubulin gene was observed in these experimental conditions; the α-tubulin gene was thus considered as a valid reference gene. Normalization was achieved for each time point by using the standard $\Delta\Delta$CT calculation method of gene expression. In the second experimental design, tubulin was no longer a valid reference gene and the NOC4 homolog gene was used for normalization. Relative expression in the GR24 treated and the control was calculated using the standard $\Delta\Delta$CT method:

$$2^{-((CT_{\text{target gene}} - CT_{NOC4})_{\text{treated}} - (CT_{\text{target gene}} - CT_{NOC4})_{\text{controls}})}.$$

All data exported from SDS 2.2 software were calculated with Microsoft Excel software. Three biological replicates were carried out in the first experimental design, and two in the second. The primer sequences used are summarized in Table II.

Supplemental Data

The following materials are available in the online version of this article.

Supplemental Figure S1. Staining of mitochondria in hyphal tips.

Supplemental Figure S2. NADH dehydrogenase activity in the presence of rotenone.

Supplemental Figure S3. Nuclear distribution in the mycelial body.

ACKNOWLEDGMENTS

The authors thank Nathalie Ladouce for her technical advice and contribution to real-time PCR experiments, Patrice Thuleau for advice in ATP content measurement by luminometry, Hélène San Clemente for assistance in bioinformatics, and Soizic Rochange and Peter Winterton for their helpful comments on the manuscript. A substantial part of this work was performed at Toulouse Rio Imaging (http://tri.ups-tlse.fr/) and in Toulouse Genopole at the genotyping/phenotyping resource center (http://genopole-toulouse.prd.fr/layout.php?page=home2&id=17&lang=fr).

Received April 17, 2008; accepted June 25, 2008; published July 9, 2008.

LITERATURE CITED

Abeles FB, Lonski J (1969) Stimulation of lettuce seed germination by ethylene. Plant Physiol **44:** 277–280

Akiyama K, Matsuzaki K, Hayashi H (2005) Plant sesquiterpenes induce hyphal branching in arbuscular mycorrhizal fungi. Nature **435:** 824–827

Andersson H, Baechi T, Hoechl M, Richter C (1998) Autofluorescence of living cells. J Microsc **191:** 1–7

Babiker AGT, Ejeta G, Butler LG, Woodson WR (1993) Ethylene biosynthesis and strigol-induced germination of Striga asiatica. Physiol Plant **88:** 359–365

Bachman NJ, Wu W, Schmidt TR, Grossman LI, Lomax MI (1999) The 5′ region of the COX4 gene contains a novel overlapping gene, NOC4. Mamm Genome **10:** 506–512

Bécard G, Fortin JA (1988) Early events of vesicular-arbuscular mycorrhiza formation on Ri T-DNA transformed roots. New Phytol **108:** 211–218

Bécard G, Pfeffer PE (1993) Status of nuclear division in arbuscular mycorrhizal fungi during in vitro development. Protoplasma **174:** 62–68

Bécard G, Piché Y (1989) New aspects on the acquisition of biotrophic status by a vesicular-arbuscular mycorrhizal fungus, *Gigaspora margarita*. New Phytol **112:** 77–83

Beilby JP (1983) Effects of inhibitors on early protein, RNA, and lipid synthesis in germinating vesicular-arbuscular mycorrhizal fungal spores of *Glomus caledonium*. Can J Microbiol **29:** 596–601

Besserer A, Puech-Pages V, Kiefer P, Gomez-Roldan V, Jauneau A, Roy S, Portais JC, Roux C, Bécard G, Séjalon-Delmas N (2006) Strigolactones stimulate arbuscular mycorrhizal fungi by activating mitochondria. PLoS Biol **4:** e226

Betz N (2007) Compatibility of the Pierce BCA protein assay with promega lysis buffers and lytic assay reagents. Promega E-Notes. http://www.promega.com/enotes/applications/ap0047_print.htm

Bouwmeester HJ, Matusova R, Zhongkui S, Beale MH (2003) Secondary metabolite signalling in host-parasitic plant interactions. Curr Opin Plant Biol **6:** 358–364

Bouwmeester HJ, Roux C, Lopez-Raez JA, Bécard G (2007) Rhizosphere communication of plants, parasitic plants and AM fungi. Trends Plant Sci **12:** 224–230

Buée M, Rossignol M, Jauneau A, Ranjeva R, Bécard G (2000) The presymbiotic growth of arbuscular mycorrhizal fungi is induced by a branching factor partially purified from plant root exudates. Mol Plant Microbe Interact **13:** 693–698

Calegario FF, Cosso RG, Fagian MM, Almeida FV, Jardim WF, Jezek P, Arruda P, Vercesi AE (2003) Stimulation of potato tuber respiration by cold stress is associated with an increased capacity of both plant uncoupling mitochondrial protein (PUMP) and alternative oxidase. J Bioenerg Biomembr **35:** 211–220

Cardenas L, McKenna ST, Kunkel JG, Hepler PK (2006) NAD(P)H oscillates in pollen tubes and is correlated with tip growth. Plant Physiol **142:** 1460–1468

Chance B, Cohen P, Jobsis F, Schoener B (1962) Intracellular oxidation-reduction states in vivo. The microfluorometry of pyridine nucleotide gives a continuous measurement of the oxidation state. Science **137:** 499–508

Cook CE, Whichard LP, Turner B, Wall ME, Egley GH (1966) Germination of witchweed (*Striga lutea* Lour.): isolation and properties of a potent stimulant. Science **154:** 1189–1190

Devin A, Rigoulet M (2007) Mechanisms of mitochondrial response to variations in energy demand in eukaryotic cells. Am J Physiol Cell Physiol **292:** C52–58

Gardes M, Bruns T (1993) ITS primers with enhanced specificity for basidiomycetes—application to the identification of mycorrhizae and rusts. Mol Ecol **2:** 113–118

Giovannetti M, Sbrana C, Logi C (1994) Early processes involved in host recognition by arbuscular mycorrhizal fungi. New Phytol **127:** 703–709

Gomez-Roldan V, Girard D, Bécard G, Puech V (2007) Strigolactones: promising plant signals. Plant Signal Behav **2:** 163–164

Gonzalez-Verdejo CI, Barandiaran X, Moreno MT, Cubero JI, Di Pietro A (2005) An improved axenic system for studying pre-infection development of the parasitic plant *Orobanche ramosa*. Ann Bot (Lond) **96:** 1121–1127

Hopper RK, Carroll S, Aponte AM, Johnson DT, French S, Shen RF, Witzmann FA, Harris RA, Balaban RS (2006) Mitochondrial matrix phosphoproteome: effect of extra mitochondrial calcium. Biochemistry **45:** 2524–2536

Horio T, Oakley BR (2005) The role of microtubules in rapid hyphal tip growth of *Aspergillus nidulans*. Mol Biol Cell **16:** 918–926

Humphrey AJ, Beale MH (2006) Strigol: biogenesis and physiological activity. Phytochemistry **67:** 636–640

Joel D, Steffens J, Matthews D (1995) Germination of weedy root parasites. *In* J Kigel, M Negbi, G Galili, eds, Seed Development and Germination. Marcel Dekker, New York, pp 567–598

Jolicoeur M, Germette S, Gaudette M, Perrier M, Bécard G (1998) Intracellular pH in arbuscular mycorrhizal fungi. A symbiotic physiological marker. Plant Physiol **116:** 1279–1288

Lanfranco L, Novero M, Bonfante P (2005) The mycorrhizal fungus *Gigaspora margarita* possesses a CuZn superoxide dismutase that is up-regulated during symbiosis with legume hosts. Plant Physiol **137:** 1319–1330

Lei J, Bécard G, Catford JG, Piché Y (1991) Root factors stimulate 32P uptake and plasmalemma ATPase activity in vesicular-arbuscular mycorrhizal fungus, *Gigaspora margarita*. New Phytol **118:** 289–294

Lemasters JJ, Hackenbrock CR (1979) Continuous measurement of adenosine triphosphate with firefly luciferase luminescence. Methods Enzymol **56:** 530–544

Liang J, Wu WL, Liu ZH, Mei YJ, Cai RX, Shen P (2007) Study the oxidative injury of yeast cells by NADH autofluorescence. Spectrochim Acta A Mol Biomol Spectrosc **67:** 355–359

Livak KJ, Schmittgen TD (2001) Analysis of relative gene expression data using real-time quantitative PCR and the 2(-Delta Delta C(T)) method. Methods **25:** 402–408

Logan DC, Stewart GR (1991) Role of ethylene in the germination of the hemiparasite *Striga hermonthica*. Plant Physiol **97:** 1435–1438

MacDonald RM, Lewis M (1978) The occurrence of some acid phosphatases and dehydrogenases in the vesicular-arbuscular mycorrhizal fungus *Glomus mossae*. New Phytol **80:** 135–141

Mandal S, Guptan P, Owusu-Ansah E, Banerjee U (2005) Mitochondrial regulation of cell cycle progression during development as revealed by the tenured mutation in Drosophila. Dev Cell **9:** 843–854

Mangnus EM, Vandenput DAL, Zwanenburg B (1992) Structural modifications of strigol analogues. Influence of the B and C rings on the bioactivity of the germination stimulant GR24. J Agric Food Chem **40:** 1222–1229

Mangnus EM, Zwanenburg B (1992) Tentative molecular mechanism for germination stimulation of *Striga* and *Orobanche* seeds by strigol and its synthetic analogues. J Agric Food Chem **40:** 1066–1070

Marcinek DJ, Schenkman KA, Ciesielski WA, Conley KE (2004) Mitochondrial coupling in vivo in mouse skeletal muscle. Am J Physiol Cell Physiol **286:** C457–463

Mayevsky A, Rogatsky GG (2007) Mitochondrial function in vivo evaluated by NADH fluorescence: from animal models to human studies. Am J Physiol Cell Physiol **292:** C615–640

McBride HM, Neuspiel M, Wasiak S (2006) Mitochondria: more than just a powerhouse. Curr Biol **16:** R551–R560

Mosse B, Hepper C (1975) Vesicular-arbuscular mycorrhizal infections in root organ cultures. Physiol Plant Pathol **5:** 215–223

Nagahashi G, Douds D Jr (1999) Rapid and sensitive bioassay to study signals between root exudates and arbuscular mycorrhizal fungi. Biotechnol Tech **13:** 893–897

Nagahashi G, Douds D Jr (2000) Partial separation of root exudate components and their effects upon the growth of germinated spores of AM fungi. Mycol Res **104:** 1453–1464

Nagahashi G, Douds D Jr (2003) Action spectrum for the induction of hyphal branches of an arbuscular mycorrhizal fungus: exposure sites versus branching sites. Mycol Res **107:** 1075–82

Nagahashi G, Douds D Jr (2007) Separated components of root exudate and cytosol stimulate different morphologically identifiable types of branching responses by arbuscular mycorrhizal fungi. Mycol Res **111:** 487–492

Navet R, Jarmuszkiewicz W, Almeida AM, Sluse-Goffart C, Sluse FE (2003) Energy conservation and dissipation in mitochondria isolated from developing tomato fruit of ethylene-defective mutants failing normal ripening: the effect of ethephon, a chemical precursor of ethylene. J Bioenerg Biomembr **35:** 157–168

Nolan T, Hands RE, Bustin SA (2006) Quantification of mRNA using real-time RT-PCR. Nat Protoc **1:** 1559–1582

Parker C (1991) Protection of crops against parasitic weeds. Crop Prot **10:** 6–22

Paszkowski U (2006) Mutualism and parasitism: the yin and yang of plant symbioses. Curr Opin Plant Biol **9:** 364–370

Pearse AGE (1968) Appendix 21. *In* Histochemistry: Theorical and Applied, Vol 2. J. and A. Churchill Ltd., London, p 1342

Peltier G, Schmidt GW (1991) Chlororespiration: an adaptation to nitrogen deficiency in *Chlamydomonas reinhardtii*. Proc Natl Acad Sci USA **88:** 4791–4795

Pfaffl MW (2001) A new mathematical model for relative quantification in real-time RT-PCR. Nucleic Acids Res **29:** e45

Popov VN, Purvis AC, Skulachev VP, Wagner AM (2001) Stress-induced changes in ubiquinone concentration and alternative oxidase in plant mitochondria. Biosci Rep **21:** 369–379

Ramos AC, Facanha AR, Feijo JA (2008) Proton (H +) flux signature for the presymbiotic development of the arbuscular mycorrhizal fungi. New Phytol **178:** 177–188

Redecker D, Thierfelder H, Walker C, Werner D (1997) Restriction analysis of PCR-amplified internal transcribed spacers of ribosomal DNA as a tool for species identification in different genera of the order Glomales. Appl Environ Microbiol **63:** 1756–1761

Remy W, Taylor TN, Hass H, Kerp H (1994) Four hundred-million-year-old vesicular arbuscular mycorrhizae. Proc Natl Acad Sci USA **91:** 11841–11843

Scheller K, Sekeris CE (2003) The effects of steroid hormones on the transcription of genes encoding enzymes of oxidative phosphorylation. Exp Physiol **88:** 129–140

Shuttleworth CW, Brennan AM, Connor JA (2003) NAD(P)H fluorescence imaging of postsynaptic neuronal activation in murine hippocampal slices. J Neurosci **23:** 3196–3208

Simon L, Bousquet J, Levesque RC, Lalonde M (1993) Origin and diversification of endomycorrhizal fungi and coincidence with vascular land plants. Nature **363:** 67–69

Smith S, Read D (1997) Mycorrhizal Symbiosis, Ed 2. Academic Press, San Diego

Spencer M, Olson AO (1965) Ethylene production and lipid mobilization during germination of castor beans. Nature **205:** 699–700

Steinberg G (2007) Hyphal growth: a tale of motors, lipids, and the Spitzenkörper. Eukaryot Cell **6:** 351–360

Sugimoto Y, Mukhtar Ali A, Yabuta S, Kinoshita H, Inanaga S, Itai A (2003) Germination strategy of *Striga hermonthica* involves regulation of ethylene biosynthesis. Physiol Plant **119:** 137–145

Tamasloukht M, Séjalon-Delmas N, Kluever A, Jauneau A, Roux C, Bécard G, Franken P (2003) Root factors induce mitochondrial-related gene expression and fungal respiration during the developmental switch from asymbiosis to presymbiosis in the arbuscular mycorrhizal fungus *Gigaspora rosea*. Plant Physiol **131:** 1468–1478

Tamasloukht M, Waschke A, Franken P (2007) Root exudate-stimulated RNA accumulation in the arbuscular mycorrhizal fungus *Gigaspora rosea*. Soil Biol Biochem **39:** 1824–1827

Weitzel J, Iwen K, Seitz H (2003) Regulation of mitochondrial biogenesis by thyroid hormone. Exp Physiol **88:** 121–128

Wu Y, Qu JY (2006) Combined depth- and time-resolved autofluorescence spectroscopy of epithelial tissue. Opt Lett **31:** 1833–1835